Biosensors and Bioelectronics 172 (2021) 112749

Contents lists available at ScienceDirect

Biosensors and Bioelectronics

journal homepage: http://www.elsevier.com/locate/bios

A CRISPR-driven colorimetric code platform for highly accurate telomerase activity assay

Meng Cheng [a], Erhu Xiong [a], Tian Tian [a], Debin Zhu [c], Huai-qiang Ju [b,*], Xiaoming Zhou [a,**]

[a] School of Life Science & College of Biophotonics, South China Normal University, Guangzhou, 510631, PR China
[b] State Key Laboratory of Oncology in South China, Collaborative Innovation Center for Cancer Medicine, Sun Yat-sen University Cancer Center, Guangzhou, 510060, PR China
[c] Guangzhou Key Laboratory of Analytical Chemistry for Biomedicine, School of Chemistry, South China Normal University, Guangzhou, 510006, China

ARTICLE INFO

Keywords:
Telomerase activity
Accuracy
Colorimetric code
CRISPR-Cas12a
CRISPR-Cas9
Lateral flow assay

ABSTRACT

Telomeric repeat amplification protocol (TRAP) has been the most widely used method for assessing the telomerase activity from cells and tissues. However, cell lysates, body fluid samples, or tumor tissue samples often contain high concentrations of protein or other complex matrices, which are usually inhibiting the TRAP response, thus leading to false-negative results. Internal control (IC) involved TRAP enables reliable telomerase activity assay but requires time consuming and laborious electrophoretic separation to visualize telomeric repeat DNA and internal control products from TRAP reaction, severely limiting its application in clinical diagnosis. Herein, a colorimetric code system based on programmable CRISPR-Cas12a technology and gold nano-particles (AuNPs) probe has been developed to analyse telomeric repeat DNA and internal control in TRAP products, enabling the rapid detection of telomerase activity and identification of false-negatives with naked-eye. We transform the detection results into three typical colorimetric codes-positive (P), negative (N) and false-negative (FN), making the judgement of detection results more convenient and user-friendly. The platform has also been applied in accurate detection of clinical liver cancer specimens for telomerase activity with a detection sensitivity of 93.75% and a specificity of 93.75% based on Youden index analysis. As a proof of concept, we further demonstrated the feasibility of Cas9-mediated triple-line lateral flow assay (TL-LFA), which enabled the detection of telomeric repeat DNA and internal control on a single triple-line test strip, achieving convenient and accurate telomerase activity assay.

Human telomerase is a ribonucleoprotein enzyme that maintains the stability of chromosomal ends of cells by adding new telomeric repeats DNA (TTAGGG) onto chromosome ends, playing a significant role in the process of cell immortalization. Significant telomerase activity can be detected in approximately 85% of primary tumours, while telomerase activity is negligible in most normal somatic cells except germ cells (Alizadeh-Ghodsi et al., 2016; Ou et al., 2019; Wu and Qu 2015; Xu et al., 2017; Zhang et al., 2017). Therefore, telomerase has been considered as an important target for clinical diagnosis and therapy of cancer. The establishment of methods for reliable and accurate detection of telomerase activity is essential for the development of new cancer diagnostic and therapeutic strategies, and would benefit the screening of telomerase-targeted anticancer drugs.

Although several methods have been developed based on nucleic acid amplification and realized sensitive detection of telomerase activity (Ma et al., 2018; Su et al., 2018; Tian and Weizmann 2013; Wang et al., 2016; Yaku et al., 2017; Zhu et al., 2014). However, their low accuracy due to the inability in identifying false-negative results severely limits the utility in analytical and clinical applications. Telomerase extracts from analytical and clinical specimens (tissues, scraped cell samples, etc.) contain complex components, including various cellular proteins and low-molecular-weight solutes, which contain DNA polymerase inhibitors, leading to the inhibition of amplification and causing false-negatives for telomerase activity assay (Herbert et al., 2006; Kim and Wu 1997; Yaku et al., 2017). Furthermore, cell samples collected from peripheral blood or scraped tissues in which telomerase activity positive cells are extremely rare or the telomerase activity is extremely weak. In this case, whole sample lysates rather than telomerase extracts

* Corresponding author.
** Corresponding author.
E-mail addresses: juhq@sysucc.org.cn (H.-q. Ju), zhouxm@scnu.edu.cn (X. Zhou).

https://doi.org/10.1016/j.bios.2020.112749
Received 20 July 2020; Received in revised form 20 September 2020; Accepted 19 October 2020
Available online 2 November 2020
0956-5663/© 2020 Elsevier B.V. All rights reserved.

are preferred when analysing tiny telomerase activity. However, whole sample lysates often contain cellular debris which is extremely adverse for amplification and will lead to false-negative diagnosis. In addition, favourable analytical tools for the screening of telomerase-targeted anticancer drugs is required because high concentration of telomerase-targeted drugs may inhibit DNA polymerase, leading to the overestimation of the drug efficiency.

Telomeric repeat amplification protocol (TRAP) has been the most widely used method for assessing the telomerase activity from cells and tissues (Herbert et al., 2006; Kim et al., 1994). In conventional TRAP, the internal standard control is incorporated to enable the identification of false-negative results arising from inhibition of DNA polymerase and errors of TRAP reagents (Kim et al., 1994; Yaku et al. 2013, 2017). Conventional TRAP requires polyacrylamide gel electrophoresis (PAGE) separation of TRAP products to check the amplicons of telomeric repeat DNA and internal control. Time consuming and tedious PAGE and post-gel operation steps greatly hinder the further application of TRAP as a diagnosis and analytical tool. Thus, the development of methods that dispense the dependence on costly laboratory equipment for reliable and rapid detection of telomerase activity is of great significance for clinical cancer diagnosis, and will greatly benefit the discovery and screening of telomerase-targeted drugs.

Clustered regularly interspaced short palindromic repeats (CRISPR) technology has been emerging as powerful bioanalytical tools for the programmable detection of nucleic acids (Chen et al., 2018; Li et al., 2018; Zhou et al., 2018). CRISPR-Cas12a is guided by a short CRISPR RNA to recognize the target double–stranded DNA (dsDNA) and forms the Cas12a/crRNA/dsDNA ternary complex, enabling the cleavage of target dsDNA (*cis*-cleavage). In addition, with the formation of ternary complex and subsequent target DNA cleavage, the *trans*-cleavage activity of Cas12a toward arbitrary single–stranded DNA (ssDNA) is also activated (Chen et al., 2018; Li et al., 2018; Yamano et al., 2017; Zetsche et al., 2015). CRISPR-Cas9 is a single RNA guided CRISPR effector; Cas9/sgRNA is capable of specific target dsDNA binding and cleavage (O'Connell et al., 2014). The sequence-specific dsDNA binding and cleavage capability of Cas9/sgRNA or dCas9/sgRNA system have been used to develop biosensors for nucleic acid assay (Guk et al., 2017; Hajian et al., 2019; Zhou et al., 2018). We recently reported a universal gene detection platform based on Cas12a and AuNP-DNA probes for colorimetric gene assay using naked-eye (Yuan et al., 2020). In addition, we also developed a Cas9/dCas9-mediated lateral flow assay (LFA) platform for nucleic acid detection (Wang et al., 2020). In the assay, Cas9/sgRNA recognizes and binds to the biotinylated dsDNA amplicons. The AuNP-DNA probes can hybridize to the loop region of the sgRNA scaffold, forming the Cas9/sgRNA/target DNA/AuNP complex. The complex can be captured by streptavidin coated in the test line of lateral flow strip, allowing visual detection of nucleic acids.

Herein, colorimetric code platforms were developed based on programmable CRISPR technology for convenient telomerase activity assay. Taking advantage of the programmable target recognition ability of Cas12a/crRNA system, crRNAs that recognize telomeric repeat DNA and Internal control were designed. Cas12a/crRNAs regulate the disperse and cross-linked state of AuNP-DNA probes in response of telomeric repeat DNA and internal control, respectively. Using this platform, we realize the detection of telomerase activity and identification of the false-negative results arising from PCR inhibitor. To make the judgement of the assay more convenient and user-friendly, the detection results were transformed into three typical colorimetric codes-positive (P), negative (N) and false-negative (FN). Furthermore, the platform was applied in the analysis of liver cancer specimens for telomerase activity. Finally, as a proof-of-concept, we also demonstrated the feasibility of Cas9-mediated TL-LFA platform for accurate telomerase activity assay. Both telomeric DNA amplicon and internal control can be analyzed on a single test strip within 15 min.

1. Experimental section

1.1. TRAP and modified TRAP

In the conventional TRAP, a volume of 2 μL telomerase extracts was added into 48 μL of TRAP reaction solution. Telomerase extension was performed at 30 °C for 30 min. The subsequent PCR program was 95 °C for 10 min; 30 cycles at 95 °C for 30 s, 59 °C for 30 s, and 72 °C for 60 s; a final extension at 72 °C for 10 min, and a 16 °C hold.

For more experimental details, please refer to the supplementary information.

2. Results and discussion

2.1. Design of the colorimetric code platform

In conventional TRAP (**Fig. 1**a), samples (cells, tissues, and body fluids) are subjected to telomerase extraction, then, cellular proteins including telomerase are released into lysis buffer, which will be used for TRAP for telomerase activity assay. Telomerase adds telomeric repeat DNA (TTAGGG) onto the 3' end of TS primer to synthesize telomerase extension products, which will be amplified in PCR step of TRAP. In addition, the TSNT (template for internal control amplification), which is incorporated to monitor the completion of TRAP, is co-amplified to generate internal control amplicons. In telomerase activity negative TRAP, only TSNT is amplified to produce internal control amplicons, indicating the success of TRAP reaction. Telomerase extracts containing inhibitors of DNA polymerase can prevent the telomerase extension product and TSNT from amplification, leading to false-negative TRAP result. Therefore, PAGE analysis of TRAP products is indispensable to visualize the internal control to rule out false-negative result, although it requires specially trained personnel, time-consuming and laborious process.

Herein, a colorimetric code platform was developed based on CRISPR-Cas12a system and AuNP-DNA probes for convenient and reliable telomerase activity assay. To achieve programmable detection of telomerase activity and TRAP internal control, crRNAs, named crRNA1 and crRNA2, targeting telomeric repeat DNA and internal control were designed. To analyse the telomeric repeat DNA and internal control from TRAP products, Cas12a/crRNA1 and Cas12a/crRNA2 mediated detection are performed, respectively. In addition, AuNP-DNA probes were implemented to the colorimetric assay. The hybridization of the terminus of ssDNA linker with DNA probes on AuNPs could cross-link AuNPs to form aggregate networks. The cross-linked AuNP-DNA probes can be easily precipitated by a short centrifugation, while the remaining AuNP-DNA monomer still keeps dispersed state, leading to a distinguishable color change of AuNPs solution.

The detection is represented by three typical colorimetric codes, that is, positive code (P), negative code (N) and false-negative code (FN), enabling rapid readout of telomerase activity assay (**Fig. 1**b). **(i)** Positive code: In the telomerase activity positive assay, Cas12a/crRNA1 can distinguish the telomeric repeat DNA amplicons from TRAP products and degrade ssDNA linker. Afterwards, AuNP-DNA probes are added into the reaction mixture. Due to the degradation of linker, AuNPs keep dispersed state and show a red color, indicating a positive telomerase activity. Furthermore, Cas12a/crRNA2 is employed to monitor internal control. Internal control activates the *trans*-cleavage activity of Cas12a/crRNA2 to degrade ssDNA linker to protect the AuNPs from cross-linking. In fact, CRISPR/crRNA1 is competent to monitor telomerase activity positive result. **(ii)** Negative code: In telomerase activity negative assay, telomeric repeat DNA amplicons are absent. Cas12a/crRNA1 mediated detection induces the cross-link of AuNPs. However, TSNT can still be amplified in telomerase activity negative TRAP. Thus, Cas12a/crRNA2 is activated by internal control to degrade ssDNA linker, keeping AuNPs in dispersed state and showing red color. **(iii)** False-negative code: In false-negative case, amplification of both telomeric repeat DNA

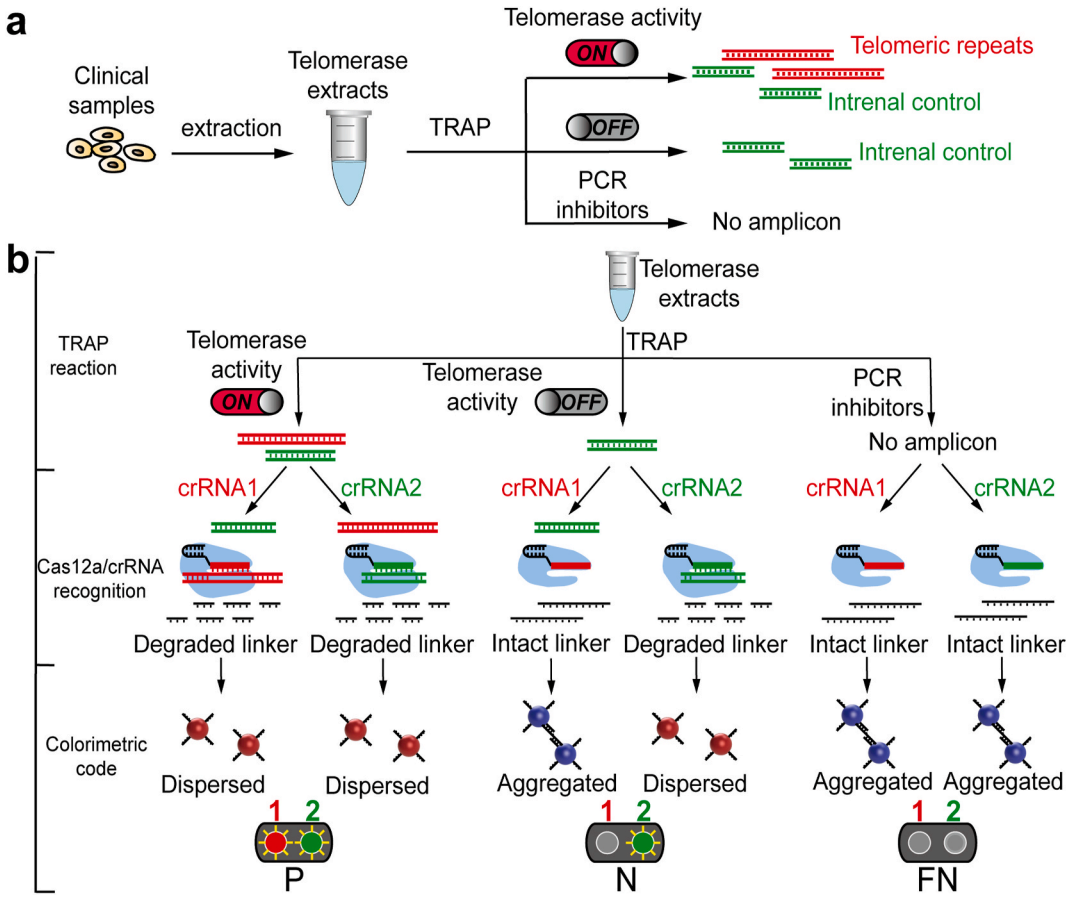


Fig. 1. **(a)** Schematic illustration of the work flow of conventional TRAP for telomerase activity assay. **(b)** Schematic illustration of colorimetric code platform for accurate telomerase activity assay. P: positive; N: negative; FN: false-negative. In colorimetric codes, light 1 represents Cas12a/crRNA1 mediated colorimetric detection, light 2 represents Cas12a/crRNA2 mediated colorimetric detection.

and internal control are abolished due to the PCR inhibitor. Thus, both Cas12a/crRNA1 and Cas12a/crRNA2 mediated analysis produced cross-linked AuNP-DNA probes to give purple color solution, indicating the false-negative TRAP result. The platform enabled the identification of false-negatives due to inhibitors of TRAP and errors of TRAP reagent, significantly improved the accuracy of conventional TRAP.

2.2. Verification of colorimetric detection platform

Fig. 2a illustrates the sequence design of crRNA1 that specifically target and distinguish telomeric repeat DNA from TRAP products. In order to design crRNA1 that aims to detect telomerase activity, telomere DNA (TTAGGG) strand of TRAP amplicon was chosen as target strand, because the sequence of the complementary strand is almost consistent with that of ACX (GCGCGGCTTACCCTTACCCTTACCCTAACC) primer, which can also activate Cas12a and lead to false result. Optimization of PAM sequence was performed and CCTA was considered to be the optimal (data not shown). TRAP experiments were performed to exam the feasibility of the colorimetric detection system for telomerase activity assay (Fig. 2b). The results showed that telomerase activity positive TRAP products activated Cas12a/crRNA1 to degrade ssDNA linker and enable AuNPs maintaining dispersed state and showing red color (Fig. S1c, S4a, S5a, c). However, in the analysis of internal control amplicons (TRAP control), the color of AuNPs changed from red to purple (Fig. S5a, c), because intact linkers promoted the formation of AuNPs aggregate networks. After a low-speed centrifugation, AuNPs of telomerase activity positive assay remained the red color, while the solution of telomerase activity negative assays displayed colorless due to the precipitation of cross-linked AuNPs (Fig. 2c). The absorbance values of the supernatant indicated the successful establishment of colorimetric detection platform for telomerase activity assay (Fig. 2d and e).

Next, we evaluated the colorimetric detection platform for the analysis of TRAP internal control. As shown in Fig. 3a, crRNA2 was designed for specific targeting of internal control in TRAP products. TRAP reactions with and without internal control were performed to test the specificity of Cas12a/crRNA2 system (Fig. 3b). The results indicated that internal control could activate Cas12a/crRNA2 to induce the ssDNA linker degradation and maintain the disperse of AuNPs, while the absence of internal control triggered the cross-linking of AuNPs to show purple color (Fig. S1c, S4b, S5b, d). We finally collected and analyzed the dispersed AuNPs after low-speed centrifugation (Fig. 3c). As displayed in Fig. 3c, the detection of TRAP products containing internal control (TRAP with IC) produced red color AuNPs solution, and analysis of absorbance spectra showed remarkable absorption signal (Fig. 3c and d). The results also showed that 0.2 fM TSNT ssDNA sequence cannot activate Cas12a to produced colorless solution, indicating that TSNT template did not affect the specificity of the assay (Fig. 3c and d). Therefore, the proposed colorimetric code platform for TRAP internal control assay revealed satisfactory specificity and feasibility.

2.3. Feasibility of the colorimetric code platform in identifying the false-negative results

The proposed colorimetric code platform was further used to monitor abnormal TRAP results. Bile salt, an inhibitor of PCR (Yaku et al. 2013, 2017), was chosen to simulate the inhibitory effect of inhibitors on TRAP reaction (Fig. S6a). As demonstrated in Fig. 4 and S6b-c, normal telomerase positive TRAP products were subjected to colorimetric assay,

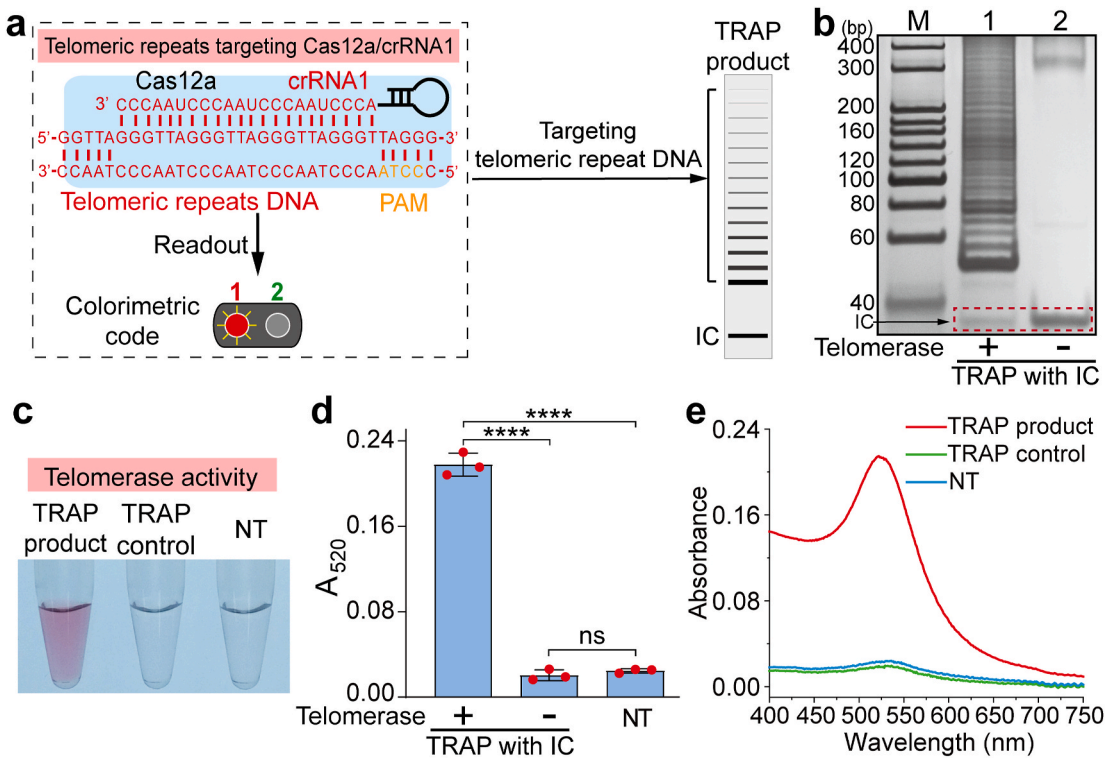


Fig. 2. The development of the colorimetric assay for telomerase activity assay. **(a)** Schematic illustration of Cas12a-AuNP system targeting telomere repeats DNA of TRAP products. **(b)** Representative PAGE analysis of TRAP amplicons. Lane 1 and 2, telomerase positive and negative TRAP products with internal control; Telomerase extracts equivalent to 100 HEK293T cells was used in telomerase positive TRAP; NP-40 lysis buffer was used as TRAP control; IC, internal control. **(c)** Verification of the colorimetric detection platform for telomerase activity assay. The concentration of AuNP–DNA probes and ssDNA linker were 3 nM and 300 nM, respectively. Measurement of A_{520} **(d)** and UV–vis absorption spectra **(e)** of the AuNPs in Fig. 2c. (n = 3 technical replicates; two-tailed Student's *t*-test; ****P < 0.0001; ns, nonsignificant; bars represent the mean ± s.d.).

both telomerase activity and internal control detection produced dispersed AuNPs, which was defined as positive result (result 1 of Fig. 4). However, in the presence of bile salt, telomerase activity and internal control detection caused AuNPs cross-linking (results 2 and 4 of Fig. 4); the absorbance values of the AuNPs confirmed the complete precipitation of cross-linked AuNPs, therefore, the false-negative was identified (Figs. S6b–c). In the TRAP negative control assay (LB, HI, RNase+, and H_2O): **(i)** Colorimetric detection of TRAP negative control (HI, RNase+, and H_2O) using Cas12a/crRNA1 caused the AuNPs cross-linking and yielded colorless supernatant (results 3 and 5-7 of Fig. 4), and only tiny absorbance signal can be detected (Fig. S6b); **(ii)** Colorimetric detection of TRAP negative control (LB, HI, RNase+, and H_2O) using Cas12a/crRNA2 produced dispersed AuNPs (results 3 and 5-7 of Fig. 4), absorbance signal assay of AuNPs solution revealed that no AuNPs probes were cross-linked (Fig. S6c); Real negative (N) results can be confirmed based on these results (**Fig. 4** and S6b-c). Notably, the addition of bile salt in telomerase activity negative TRAP also produced false-negative (FN) readout (result 4 of **Fig. 4**). Such phenomenon indicated the abnormal TRAP, reminding further adjustment of sample examination to rule out false-negative results. These results demonstrated that we have successfully established a colorimetric code platform to identify the false-negative TRAP results due to PCR inhibitors.

2.4. Detection performance of the colorimetric code platform

We evaluated the detection sensitivity of the proposed platform for telomerase activity. The method can detect telomerase activity equivalent to 1 HEK293T cell, 1 Hela cell and 5 A549 cells, respectively (Fig. S7). These results demonstrated the universality and high sensitivity of the proposed system for telomerase activity assay.

The latest survey showed that liver cancer has become one of the highest mortality cancers (Bray et al., 2018). We applied the method in the analysis of clinical liver cancer specimens. As shown in **Fig. 5**a, S8a and c, telomerase activity was detectable in almost all the cancer tissues and one of the cancer adjacent tissues, while cancer tissue No. 5 showed negative telomerase activity. The internal control assays precluded false-negative results (**Fig. 5**b, S8b and d). Notably, positive telomerase activity was detected in cancer adjacent tissue No. 11 (**Fig. 5**a, S8a and c). Such result may attribute to the incomplete resection of the tumor tissue, or indicate that the patient may have a poor prognosis due to higher recurrence rate (Singhal et al., 2012). As demonstrated in **Fig. 5**c, the receiver operating characteristic (ROC) analysis was performed to evaluate the results of the colorimetric assay (AUC = 0.9648). Based on the Youden index assay, the detection specificity of 93.75% and sensitivity of 93.75% were achieved using the colorimetric assay. In addition, a comparison between the colorimetric assay and conventional RQ-TRAP (Fig. S9) indicates that the accuracy of the proposed platform (AUC = 0.9648) is superior to that of the conventional RQ-TRAP method (AUC = 0.9492). These results indicated that proposed method has the potential for further application in clinical diagnosis and postoperative prognosis evaluation.

Finally, the feasibility of isothermal amplification-based colorimetric assay was evaluated. Wang et al. has reported stem-loop primer-mediated exponential amplification (SPEA) for isothermal amplification of telomerase extension products and produced dsDNA amplicons, achieved high-sensitive telomerase activity assay (Fig. S10a) (Wang et al., 2016). SPEA was adopted for isothermal amplification-based colorimetric assay of telomerase activity. The results showed that obvious DNA ladder amplicons were produced by SPEA in response of synthetic template and telomerase, while negative control SPEA reaction did not generate any DNA ladder product (Fig. S10b). Cas12a-mediated colorimetric assay of the SPEA product displayed that the detection of

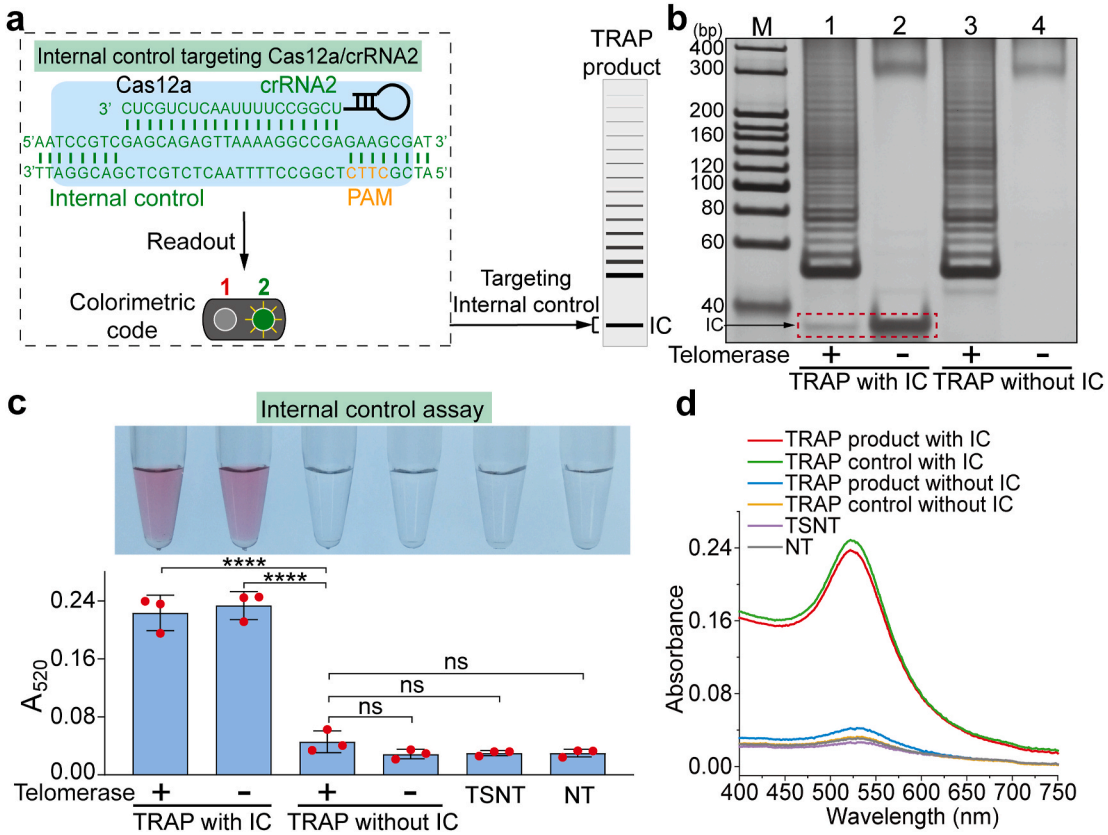


Fig. 3. The development of the colorimetric detection platform for internal control assay. **(a)** Schematic illustration of Cas12a-GNP system targeting internal control sequence of TRAP products. **(b)** Representative PAGE analysis of TRAP amplicons. Lane 1 and 2, telomerase positive and negative TRAP products with internal control; Lane 3 and 4, telomerase positive and negative TRAP products without internal control; Telomerase extracts equivalent to 100 HEK293T cells were used in telomerase positive TRAP reaction; NP-40 lysis buffer was used as TRAP control; 0.2 fM of TSNT ssDNA was used in TRAP with IC; TSNT ssDNA sequence was absent in TRAP without IC; IC, internal control. **(c)** Top: photograph of the colorimetric detection results of the internal control from TRAP products. Bottom: measurement of A_{520} value of the AuNPs. The concentration of AuNP–DNA probes and ssDNA linker were 3 nM and 300 nM, respectively. **(d)** Measurement of UV–vis absorption spectra of the AuNPs in Fig. 3c. (n = 3 technical replicates; two-tailed Student's *t*-test; ****P < 0.0001; ns, nonsignificant; bars represent the mean ± s.d.).

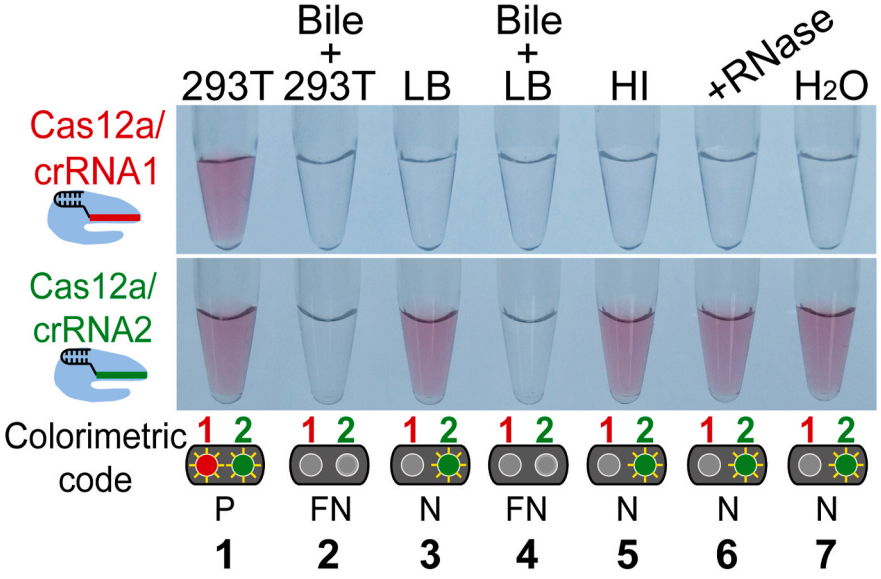


Fig. 4. Colorimetric detection platform monitors false-negative TRAP results. Colorimetric assay of TRAP products: 1, telomerase positive TRAP; 2, telomerase positive TRAP in the presence of bile; 3, telomerase negative TRAP; 4, telomerase negative TRAP in the presence of bile salt; 5, HI (heat-inactivated telomerase); 6, +RNase (RNase-treated telomerase); 7, H_2O was used in TRAP control; Telomerase extracts equivalent to 100 HEK293T cells were used in the telomerase positive TRAP; 1.5 μg/μL of bile salt was used to stimulate inhibited TRAP reactions; IC, internal control. Colorimetric code: P, positive; N, negative; FN, false-negative. The concentration of AuNP–DNA probes and ssDNA linker were 3 nM and 300 nM, respectively.

telomerase activity positive SPEA amplicon produced colored AuNP solution, and the colorless AuNP supernatant was obtained in the analysis of telomerase negative sample (Fig. S10c). These results demonstrated the application potential of current colorimetric code platform in point-of-care (POC) diagnosis.

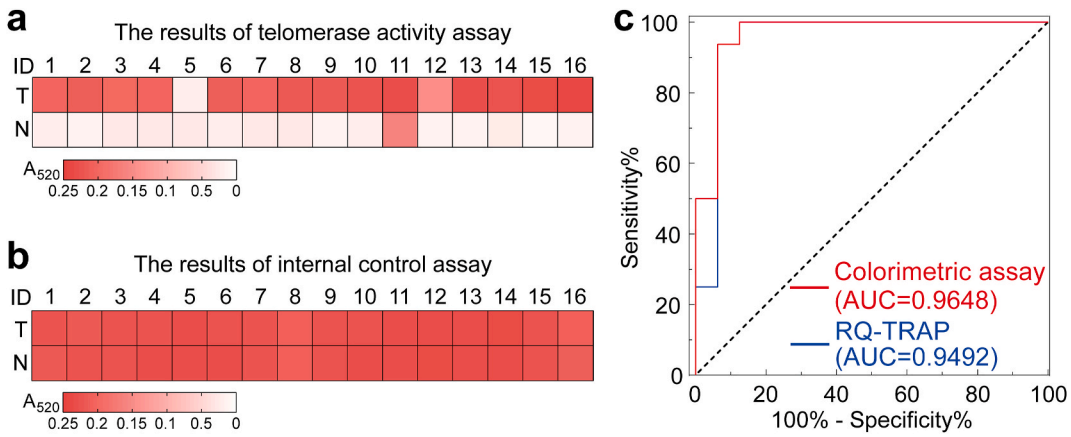


Fig. 5. Telomerase activity assay of clinical liver cancer tissue specimens. Colorimetric assay results for telomerase activity **(a)** and TRAP internal control **(b)**. **(c)** ROC curve of telomerase activity detection was generated to evaluate the detection accuracy of the colorimetric detection platform and conventional RQ-TRAP. ID, sample ID; T, tumor; N, normal.

2.5. Detection principle of the LFA-Based colorimetric code platform

CRISPR-Cas9 has shown the great potential in the development of programmable DNA biosensors (Wang et al., 2020; Zhou et al., 2018). Herein, as a proof-of-concept, we demonstrated the feasibility of our colorimetric code concept by developing Cas9-mediated TL-LFA platform. As illustrated in **Fig. 6**a, the engineered TL-lateral flow device was composed of sample pad, conjugate pad, test line 1 and 2, control line, and absorbent pad. AuNP-DNA probes were precoated in the conjugate pad. The DNA probes, which were immobilized on AuNP through the affinity between Au and poly A (adenine) sequence, containing a sgRNA binding region and a control line hybridization region (Fig. S11). Streptavidin and anti-FITC antibody were precoated in the test line 1 and test line 2, respectively. Streptavidin-biotin-probe 1 was immobilized in the control line to capture excess AuNP-DNA probes.

Two specific sgRNAs (sgRNA1 and sgRNA2) were designed for the assay (**Fig. 6**a, S11a-b). Cas9/sgRNA1 and Cas9/sgRNA2 can discriminate and bind to telomeric repeat DNA and internal control from TRAP products, respectively. The loop structure in the scaffold of the sgRNA contains a sequence that can hybridize with the sgRNA binding region of AuNP-DNA probes. Cas9 protein is a single turnover nuclease (Sternberg et al., 2015). The Cas9/sgRNA releases the target dsDNA under extremely low rate after cleavage (Ma et al., 2016), thus forming the stable Cas9/sgRNA/target complex. When the Cas9 reaction mixture is instilled on the sample pad of the test strip, the capillarity force propels the Cas9/sgRNA/target complex to flow into the conjugate pad region, where the AuNP-DNA probes anchor to the loop region of sgRNA and form AuNP/Cas9/sgRNA/target complex (**Fig. 6**a). The formed complex and excess AuNP probes further flow laterally through the test line and control line. Biotinylated AuNP/Cas9/sgRNA1/telomeric repeat DNA complex can be captured by streptavidin in test line 1, while FITC labeled AuNP/Cas9/sgRNA2/internal control DNA complex is intercepted by anti-FITC antibody in test line 2. Excess AuNP probes are captured in the control line (**Fig. 6**a, S11c-d). With the accumulation of AuNPs, colored bands can be observed for visual detection of telomerase activity, achieving LFA-based colorimetric code system.

TRAP experiments using modified TS and ACX primers were performed to test the function of the modified TRAP primers. As shown in **Fig. 6**b, with the use of modified primers, PAGE analysis of TRAP amplicons produced typical 6-bp telomeric DNA ladder (lane 1, 5), which was similar with that produced by conventional TRAP (lane 3, 7). These results indicated that the modified primer Biotin-ACX showed normal function. In addition, TRAP using FITC-NT primer produced relatively larger TSNT amplicon (internal control) in comparison with that of conventional TRAP (lane 1–4). This may result from the incorporation of the FITC in TSNT amplicon. Subsequently, the function of the proposed LFA system for the detection of modified TRAP products was evaluated. As displayed in **Fig. 6**b and S12a, in the presence of biotinylated telomeric DNA amplicon, evident colored bands can be observed in the test line 1 (result 1 of Fig. 6b), while conventional TRAP amplicon did not induce any accumulation of AuNPs in test line 1 (results 3, 5 and 7 of Fig. 6b). In addition, large amount of telomeric repeat DNA amplicon did not cause any non-specific color change in test line 2 (results 1, 3, 5 and 7 of Fig. 6b). These results revealed that the test line 1 of the TL-LFA strip can be used for specific telomeric repeat DNA detection, allowing specific telomerase activity assay. Furthermore, the feasibility of the TL-LFA platform for the monitoring of TRAP internal control was also evaluated. As demonstrated in **Fig. 6**b, a colored band appeared in the test line 2 region in response of the FITC-labeled internal control amplicon, while conventional internal control amplicon and telomeric DNA amplicon did not lead to any color change in test line 2 (result 2 of **Fig. 6**b and S12a). These results revealed the feasibility and specificity of the TL-LFA platform for the monitoring of TRAP internal control.

2.6. LFA-based colorimetric code platform identified false-negative TRAP

Next, TRAP inhibition experiments were conducted to check the ability of the TL-LFA biosensor for the identification of false-negative TRAP results. Bile salt was used to simulate the typical false-negative TRAP results, which were identical to that shown in Fig. S6a. As shown in result 1 of **Fig. 6**c and S12b, the analysis of normal telomerase activity positive TRAP product produced obvious band in test line 1, which was defined as positive code (P). However, the introduction of inhibitor in telomerase positive TRAP led to the absence of colored band in both test line 1 and 2 (result 2 of **Fig. 6**c and S12b). The presence of the control line band revealed the normal function of the test strip, thus confirming the false-negative TRAP result, producing a typical false-negative code (FN). The detection of telomerase activity negative TRAP product obtained normal negative code (N), in which colored bands appeared in test line 2 while test line 1 did not display any color change (result 3, 5–7 of **Fig. 6**c and S12b). Noticeably, bile salt inhibited the telomerase activity negative TRAP and generated false-negative result (result 4 of **Fig. 6**c and S12b), indicating the presence of inhibitors or abnormal TRAP. These results demonstrated the feasibility of TL-LFA-based colorimetric code platform for accurate telomerase activity assay. Furthermore, the assay can be completed within 15 min, showing great potential for rapid and convenient analysis of complex clinical samples for telomerase activity.

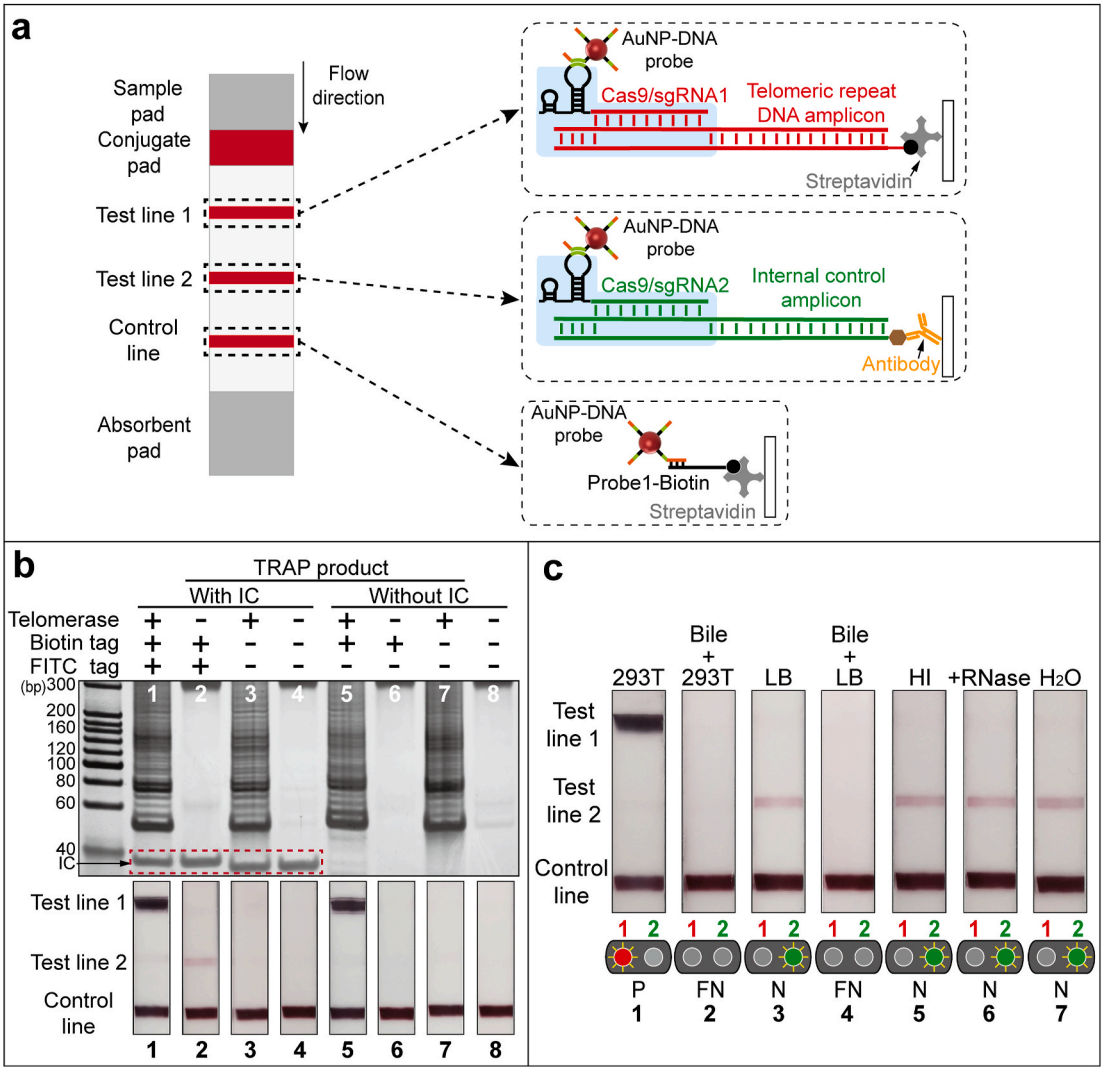


Fig. 6. Demonstration of the applicability of the colorimetric code strategy based on TL-lateral flow assay platform for accurate telomerase activity assay. **(a)** Schematic illustration of CRIPSR/Cas9-mediated TL-LFA platform. **(b)** Top panel: PAGE analysis of conventional and modified TRAP products. Bottom panel: Verification of Cas9-mediated TL-LFA platform for specific detection of telomeric DNA amplicon and internal control from TRAP product. Biotin tag +: Biotin-ACX primer was used instead of ACX primer; FAM tag +: FAM-NT primer was used instead of NT primer. 0.2 fM of TSNT was used in TRAP with IC, TSNT ssDNA was not added in TRAP without IC. **(c)** Cas9 mediated TL-LFA platform was used to analyse TRAP products: 1, telomerase positive TRAP; 2, telomerase positive TRAP in the presence of bile; 3, telomerase negative TRAP; 4, telomerase negative TRAP in the presence of bile salt; 5, HI (heat-inactivated telomerase); 6, +RNase (RNase-treated telomerase); 7, H_2O was used in TRAP control; 1.5 μg/μL of bile salt was used to simulate inhibited TRAP reactions; IC, internal control. Colorimetric code: P, positive; N, negative; FN, false-negative. Telomerase extracts equivalent to 500 HEK293T cells were used in telomerase positive TRAP; Lysis buffer was used in telomerase negative control TRAP.

3. Conclusions

In this work, we proposed a colorimetric code platform based on TRAP and CRISPR-Cas12a technology for the reliable telomerase activity assay using naked eye. The platform successfully identified false-negative result arising from the PCR inhibitors. The colorimetric assay was proved to be compatible with isothermal amplification-based telomerase activity assay. We also demonstrated the feasibility of Cas9-mediated TL-LFA platform for convenient and reliable telomerase activity assay. In summary, the proposed system possesses several advantages comparing with previous methods. (i) Accurate and convenient visual detection of telomerase activity without the requirement of PAGE. (ii) Cas9-mediated triple-line LFA platform detects both telomerase activity and internal control on a single test strip. (iii) The colorimetric code strategy is compatible with isothermal amplification, allowing the development of point–of–care diagnostics for telomerase activity assay. A comparison between the proposed strategy and previous method is displayed in Table S2. We hope that the proposed strategy will be widely adopted in the field of biomedical study and clinical cancer diagnosis.

CRediT authorship contribution statement

Meng Cheng: conceived of the presented idea, conceived and planned the experiments, carried out almost all the experiments. **Erhu Xiong:** prepared the AuNP and AuNP-DNA probes. **Tian Tian:** expressed and purified all Cas proteins. **Debin Zhu:** prepared and analyzed the clinical samples. **Huai-qiang Ju:** conceived and planned the experiments, prepared and analyzed the clinical samples. **Xiaoming Zhou:** conceived of the presented idea, conceived and planned the experiments, All authors discussed the results and contributed to the final manuscript.

Declaration of competing interest

The authors declare that they have no known competing financial interests or personal relationships that could have appeared to influence the work reported in this paper.

Acknowledgments

We thank the National Natural Science Foundation of China (Grant 21874049; 91959128; 21904042; 81772246), the Special Support Program of Guangdong Province (Grant 2016TQ03R749), the Special Project of the Science and Technology Development of Guangdong Province (2017B020207011), and the Open Funds of the State Key Laboratory of Electroanalytical Chemistry (SKLEAC202001).

Appendix A. Supplementary data

Supplementary data to this article can be found online at https://doi.org/10.1016/j.bios.2020.112749.

References

Alizadeh-Ghodsi, M., Zavari-Nematabad, A., Hamishehkar, H., Akbarzadeh, A., Mahmoudi-Badiki, T., Zarghami, F., Pourhassan Moghaddam, M., Alipour, E., Zarghami, N., 2016. Biosens. Bioelectron. 80, 426–432.
Bray, F., Ferlay, J., Soerjomataram, I., Siegel, R.L., Torre, L.A., Jemal, A., 2018. CA Canc. J. Clin. 68 (6), 394–424.
Chen, J.S., Ma, E., Harrington, L.B., Da Costa, M., Tian, X., Palefsky, J.M., Doudna, J.A., 2018. Science 360 (6387), 436–439.
Guk, K., Keem, J.O., Hwang, S.G., Kim, H., Kang, T., Lim, E.-K., Jung, J., 2017. Biosens. Bioelectron. 95, 67–71.
Hajian, R., Balderston, S., Tran, T., deBoer, T., Etienne, J., Sandhu, M., Wauford, N.A., Chung, J.-Y., Nokes, J., Athaiya, M., Paredes, J., Peytavi, R., Goldsmith, B., Murthy, N., Conboy, I.M., Aran, K., 2019. Nat. Biomed. Eng. 3 (6), 427–437.
Herbert, B.S., Hochreiter, A.E., Wright, W.E., Shay, J.W., 2006. Nat. Protoc. 1 (3), 1583–1590.
Kim, N., Piatyszek, M., Prowse, K., Harley, C., West, M., Ho, P., Coviello, G., Wright, W., Weinrich, S., Shay, J., 1994. Science 266 (5193), 2011–2015.
Kim, N.W., Wu, F., 1997. Nucleic Acids Res. 25 (13), 2595–2597.
Li, S.-Y., Cheng, Q.-X., Liu, J.-K., Nie, X.-Q., Zhao, G.-P., Wang, J., 2018. Cell Res. 28 (4), 491–493.
Ma, F., Wei, S.H., Leng, J., Tang, B., Zhang, C.Y., 2018. Chem. Commun. 54 (20), 2483–2486.
Ma, H., Tu, L.-C., Naseri, A., Huisman, M., Zhang, S., Grunwald, D., Pederson, T., 2016. J. Cell Biol. 214 (5), 529–537.
O'Connell, M.R., Oakes, B.L., Sternberg, S.H., East-Seletsky, A., Kaplan, M., Doudna, J.A., 2014. Nature 516 (7530), 263–266.
Ou, X., Zhan, S., Sun, C., Cheng, Y., Wang, X., Liu, B., Zhai, T., Lou, X., Xia, F., 2019. Biosens. Bioelectron. 124–125, 199–204.
Singhal, A., Jayaraman, M., Dhanasekaran, D.N., Kohli, V., 2012. Crit. Rev. Oncol. Hematol. 82 (2), 116–140.
Sternberg, S.H., LaFrance, B., Kaplan, M., Doudna, J.A., 2015. Nature 527 (7576), 110–113.
Su, D., Huang, X., Dong, C., Ren, J., 2018. Anal. Chem. 90 (1), 1006–1013.
Tian, L., Weizmann, Y., 2013. J. Am. Chem. Soc. 135 (5), 1661–1664.
Wang, H., Wang, H., Liu, C., Duan, X., Li, Z., 2016. Chem. Sci. 7 (8), 4945–4950.
Wang, X., Xiong, E., Tian, T., Cheng, M., Lin, W., Wang, H., Zhang, G., Sun, J., Zhou, X., 2020. ACS Nano 14 (2), 2497–2508.
Wu, L., Qu, X., 2015. Chem. Soc. Rev. 44 (10), 2963–2997.
Xu, X., Wei, M., Liu, Y., Liu, X., Wei, W., Zhang, Y., Liu, S., 2017. Biosens. Bioelectron. 87, 600–606.
Yaku, H., Murashima, T., Miyoshi, D., Sugimoto, N., 2013. Molecules 18 (10), 11751–11767.
Yaku, H., Yoshida, Y., Okazawa, H., Kiyono, Y., Fujita, Y., Miyoshi, D., 2017. Anal. Chem. 89 (13), 6948–6953.
Yamano, T., Zetsche, B., Ishitani, R., Zhang, F., Nishimasu, H., Nureki, O., 2017. Mol. Cell. 67 (4), 633–645.
Yuan, C., Tian, T., Sun, J., Hu, M., Wang, X., Xiong, E., Cheng, M., Bao, Y., Lin, W., Jiang, J., Yang, C., Chen, Q., Zhang, H., Wang, H., Wang, X., Deng, X., Liao, X., Liu, Y., Wang, Z., Zhang, G., Zhou, X., 2020. Anal. Chem. 92 (5), 4029–4037.
Zetsche, B., Gootenberg, J.S., Abudayyeh, O.O., Slaymaker, I.M., Makarova, K.S., Essletzbichler, P., Volz, S.E., Joung, J., van der Oost, J., Regev, A., Koonin, E.V., Zhang, F., 2015. Cell 163 (3), 759–771.
Zhang, X., Lou, X., Xia, F., 2017. Theranostics 7 (7), 1847–1862.
Zhou, W., Hu, L., Ying, L., Zhao, Z., Chu, P.K., Yu, X.-F., 2018. Nat. Commun. 9 (1), 1–11.
Zhu, X., Xu, H., Lin, R., Yang, G., Lin, Z., Chen, G., 2014. Chem. Commun. 50 (58), 7897–7899.